Decomposing Three-Dimensional Shapes into Self-supporting, Discrete-Element Assemblies

Ursula Frick, Tom Van Mele and Philippe Block

Abstract

This study investigates a computational design approach to generate volumetric decompositions of given, arbitrary, three-dimensional shapes into self supporting, discrete-element assemblies. These assemblies are structures formed by individual units that remain in equilibrium solely as a result of compressive and frictional contact forces between the elements. This paper presents a prototypical implementation of a decomposition tool into a CAD software, focusing on user-controlled design to generate such assemblies. The implementation provides an interactive design environment including real time visual feedback, in which the design space of self-supporting block assemblies can be explored and expanded. Some surprising results of such explorations are included and discussed.

Introduction

Volumetric decomposition as a means to reduce element size in assemblies is relevant to the building industry because it simplifies fabrication and transport. The connections between the individual units needed to establish equilibrium of the assembly are often problematic, material intensive or complicated. Especially tensile, mechanical connections often result in complicated detailing and can be expensive and intrusive. Glued connections are mainly simple, but typically difficult to adjust or remove.

This research presents a prototypical decomposition tool as a means to design volumetric decomposition of three-dimensional shapes into self-supporting, discrete-element assemblies. The generated structures, formed by individual, disjoint units, rely solely on spatial compression flows (arching), friction, balancing, and any combination of these actions to stand in equilibrium (Fig. 1). This means they are stable without additional mechanical or physical joinery between the blocks, which keeps the connections simple and adjustable.

Considering the structural integrity of such assemblies, the defining principles that must be evaluated are the assembly's overall stability and

U. Frick (✉) · T.V. Mele · P. Block
Block Research Group, ETH Zurich Institute of
Technology in Architecture, Zurich, Switzerland
e-mail: frick@arch.ethz.ch

Fig. 1 Photographs of a discrete element assembly in equilibrium as a result of arching, friction, and balancing, and without mechanical connections or glue

material failure at the scale of the individual unit. As stability is predominantly an issue of geometry and not of internal stress distributions, methods to address geometrical stability are embedded in the presented computational setup. Material failure of the discrete elements is not considered at this stage of the research.

Related Work

Discretization of architectural geometries and design of self-supporting structures are ongoing and active areas of research. Both topics play an important role in architectural design and associated fields and have a strong influence on manufacturing, assembly and building cost.

In recent years, various innovative computational techniques for topological and surface-based discretization of architectural geometries have been developed, such as Pottmann et al. (2008) and Eigensatz et al. (2010). However, few of these techniques consider structural and/or assembly constraints e.g. Rippmann et al. (2013), Panozzo et al. (2013) and Deuss et al. (2014). Furthermore, in most cases topological and surface based discretization approaches are not applicable to volumetric shapes.

Most existing volumetric discretization approaches, such as methods to decompose solids into parts optimized for layered fabrication (Hu et al. 2014), do not consider interactions that keep disjoint assemblies in equilibrium. Whiting et al. (2009), Whiting (2012) presented an approach for generating structurally sound masonry assemblies by refining coarse volumetric models with known/typical structural elements such as walls, arches, domes, etc.

Objectives and Outline

The presented approach focuses on interactive decomposition of given arbitrary shapes that would naturally not be considered as suitable shapes for self-supporting, discrete-element structures. By providing *real-time* visual feedback, it allows exploring and extending the design space of such assemblies. From this design perspective, the proposed approach offers a means of creating surprising equilibrium assemblies that go beyond the scope of known structurally sound configurations for unreinforced masonry and other discrete-element structures.

"*Decomposition process*" gives an overview of the decomposition process, the used structural analysis method and the computational implementation. In "*Results*", the results of explorations are presented with three case studies. The stability of the generated digital models are validated with 3D-printed physical models and illustrated with photographs. "Conclusion" discusses the presented approach and gives an outlook to future work.

Decomposition Process

This section gives an overview of a prototypical implementation of a decomposition tool in Rhinoceros (2014). Grasshopper (2009) was used to build up an interactive design environment. Equilibrium calculations were written in Python (2015) and solved with quadratic programming.

The decomposition process starts with an initial geometry, which is refined step by step until a satisfactory result is obtained. After every user-controlled refinement, interfaces between blocks, and between blocks and the surroundings are detected automatically. At every step, the discretization of the geometry can be changed or updated, whereafter no-tension equilibrium has to be (re-)established. An equilibrium solution can be found by changing the boundary conditions, modifying the location and orientation of the interfaces, changing the material properties, or any combination of these options. Providing intuitive, visual feedback on the current state of the model is clearly essential during this process.

Equilibrium Calculation

The equilibrium calculations are based on the method described in Whiting (2012) and Whiting et al. (2009, 2012).This method extends the Rigid Block Limit Equilibrium Analysis method by Livesley (1978, 1992) by including penalty forces to allow for configurations of discrete-element assemblies in which tension is required. This structural analysis method enables computing estimates of the occurring forces in a given structure that satisfy the equilibrium equations, including friction constraints, with quadratic programming.

Here, we briefly summarize the essential equations of the optimization problem. The static equilibrium equations (Whiting et al. 2009) can be set up in matrix form as follows:

$$A_{eq} * c + b = 0$$

The matrix A_{eq} contains the sub-matrices $A_{j,k}$ of size $6 \times 4 v_k$, with v_k the number of vertices of interface k, representing the (global) xyz-components of the force and moment interactions between block j and interface k in the local coordinate system $(\hat{n}_k, \hat{u}_k, \hat{v}_k)$ of interface k (Fig. 2):

$$A_{j,k} * c_k + b_j = 0$$

which expands to:

$$
\begin{bmatrix}
f_{kx} & f_{kx} & & f_{kx} \\
f_{ky} & f_{ky} & & f_{ky} \\
f_{kz} & f_{kz} & & f_{kz} \\
m^1_{j,k_x} & m^2_{j,k_x} & \cdots & m^v_{j,k_x} \\
m^1_{j,k_y} & m^2_{j,k_y} & & m^v_{j,k_y} \\
m^1_{j,k_z} & m^2_{j,k_z} & & m^v_{j,k_z}
\end{bmatrix}
*
\begin{bmatrix}
c^1_k \\
c^2_k \\
\vdots \\
c^{v_k}_k
\end{bmatrix}
+
\begin{bmatrix}
F_{jx} \\
F_{jy} \\
F_{jz} \\
M_{jx} \\
M_{jy} \\
M_{jz}
\end{bmatrix}
$$
$$= 0$$

The sub-vectors f_{kx}, f_{ky}, and f_{kz} of $A_{j,k}$ contain the xyz-components of the local coordinate system of interface k.

$$f_{kx} = \left[(\hat{n}_k)_x, -(\hat{n}_k)_x, (\hat{u}_k)_x, (\hat{v}_k)_x \right]$$

The sub-vectors m^i_{j,k_x}, m^i_{j,k_y} and m^i_{j,k_z} contain the xyz-components of the moment contributions of the interface forces of vertex i of interface k,
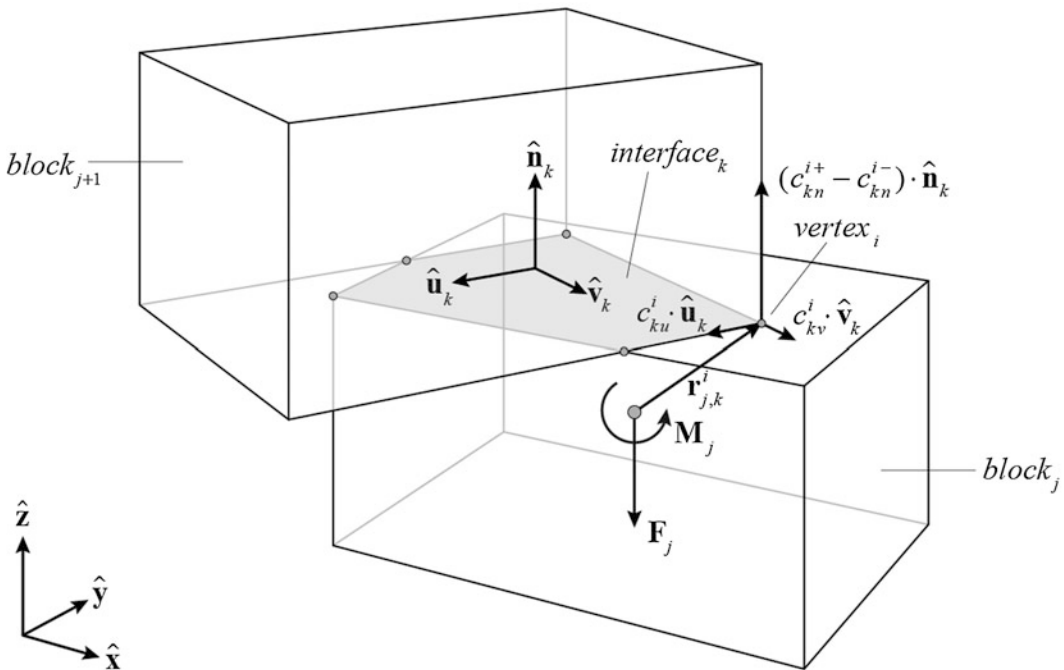

Fig. 2 Diagram of the interaction between block j and interface k

acting on block j. The vector $r_{j,k}^i$ defines the relative position of vertex i with respect to the mass centroid of block j.

$$m_{j,k_x}^i = \left[(r_{j,k}^i \times \hat{n}_k)_{x,} - (r_{j,k}^i \times \hat{n}_k)_{x,} (r_{j,k}^i \times \hat{u}_k)_{x,} (r_{j,k}^i \times \hat{v}_k)_x \right]$$

The $4_{vk} \times 1$ vector c_k, with v_k the number of vertices of interface k, contains the unknown normal and in-plane force coefficients (signed force magnitudes) for all vertices of interface k, including the penalty formulation as described in Whiting et al. (2009), Whiting (2012).

$$\begin{aligned} c_{normal} &= c_n^+ - c_n^- \\ c_{friction} &= c_u + c_v \end{aligned} \Rightarrow c_k^i = \begin{bmatrix} c_{kn}^{i+} \\ c_{kn}^{i-} \\ c_{ku}^{i} \\ c_{kv}^{i} \end{bmatrix}$$

The 6×1 sub-vector b_j contains the xyz-components of the body forces applied to the centroid of block j.

To improve stability of the calculation, an eight-sided friction pyramid (Livesley 1992) rather than the four-sided one used in Whiting (2012) has been used for friction constraints (μ is the static friction coefficient of the used material).

$$\left(|c_u|, \ |c_v|, \ \frac{1}{\sqrt{2}} |c_u| + \frac{1}{\sqrt{2}} |c_v| \right) \le \mu * c_n^{c+}$$

The energy function, as described in Whiting (2012), has then been used to calculate the interface-forces.

$$\underset{c}{minimize} \ f(c) \ such \ that \begin{cases} A_{eq} * c = -b \\ c_{normal} \ge 0 \\ c_{friction} \le \mu * c_n^+ \end{cases}$$

This structural analysis method enables the calculation of infeasible self-supporting structures. Infeasible self-supporting structures are those for which the no-tension equilibrium is violated. In comparison, stability simulations with physics engines, e.g. Bullet-Physics-Library (2012) and Nvidia physx library (2013), would typically result in a Yes/No answer. Furthermore, the equilibrium equations of the used method can be solved reasonably prompt with quadratic programming. Both of these points makes the approach particularly adequate to be implemented into a computational setup with emphasis on interactivity.

Interface-Force Diagrams

The models are visualized using interface-force diagrams, in which contact interfaces are represented by coloured surfaces. The colours provide different information about the forces at the interfaces depending on the selected feedback mode.

In compression-tension mode, blue indicates compression, and red tension. Colour gradients indicate variations in the distribution of forces over the interface and interfaces without compression are grey. Note, that the colour gradients represent the force distribution normalized per face and do not reflect the force magnitudes. Relative contact-force magnitudes are visualized by switching to vector mode.

In friction mode, interfaces without friction are also grey. Interfaces with friction have solid colours between yellow and red. All friction forces below a user-defined threshold are illustrated in yellow. Red indicates that the friction force exceeds the allowed maximum. Occurring friction forces between those bounds are illustrated with orange shades. For example, dark orange indicates that the resulting friction force is close to the allowed maximum.

For easier understanding of the assembly's equilibrium, mass-center locations are displayed and additional information of contact-force magnitudes in text form are optional. Figures 3, 4 and 5 illustrate the gradient and vector visualizations modes and the influence of user-controlled modifications.

Feedback and Equilibrium Modification

Figure 3 depicts different configurations of a solid object in the shape of the letters SC. The interfaces are shown in compression-tension mode. In Fig. 3a, the notension constraint is violated at the support interfaces. The left support is entirely in tension. At the right support interface, both tension and compression forces occur simultaneously. This equilibrium is the result of the location of the center of mass of the shape in relation to the supports. No-tension equilibrium can be established by adding an additional support interface (Fig. 3b), or by changing the overall geometry (Fig. 3c).

Figures 4 and 5 depict different configurations of a discretization of the letter "M". Figure 4 shows the interfaces in compression-tension mode. In configuration a, no-tension equilibrium is violated due to the need for tension forces at the internal interface (between the top and bottom element). In configurations b and c, the violation is resolved by changing the location of the cut. The colour gradient in Fig. 4b indicates that, at this location, the compression forces are unevenly distributed over the interface. Moving the cut further down results in a more even

distribution and thus a more robust equilibrium (Fig. 4c). Note that in all cases compression forces at the support interface are evenly distributed, as these forces depend only on global equilibrium, which remains unaltered in the three cases. Figure 5 shows the interfaces of a slightly different discretization of the M-shaped object in friction mode. In configuration a, the orientation of the cut is such that maximum friction is exceeded. By rotating the cut in configurations b and c, friction is reduced to allowable levels. Friction is lowest in configuration c. Note that in none of the configurations friction occurs at the support interface, since the applied loads are vertical and there is no arch action.

Results

This section presents the results of explorations of the no-tension discrete-element assembly design space with the decomposition tool discussed in "*Decomposition process*". The equilibrium of the generated digital models has been verified with physical models. The physical models were 3D printed with a ZCORP ZPrinter 650, using a composite of zp150 powder and
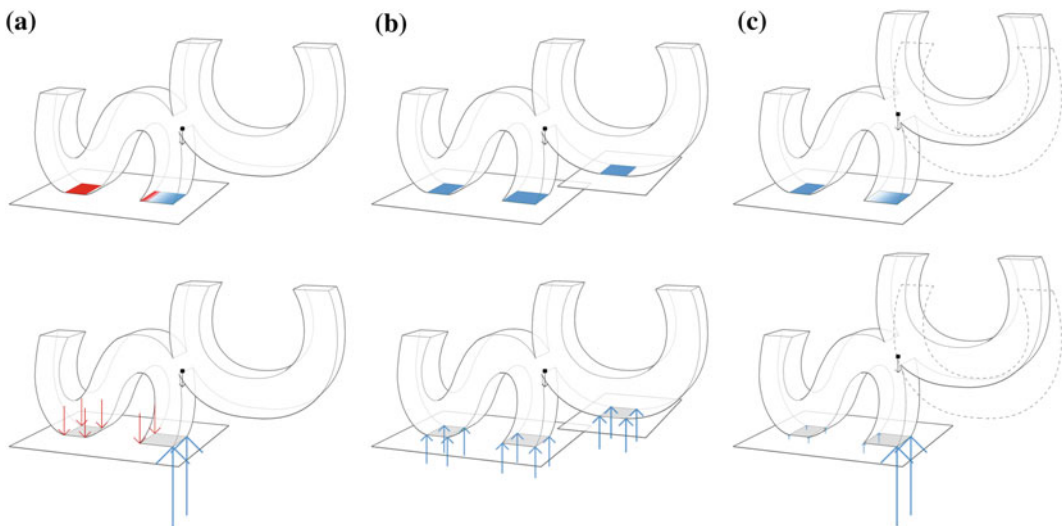
Fig. 3 Different configurations of a solid object in the shape of the letters SC. **a** Violation of no-tension equilibrium at the support. No-tension equilibrium established by (**b**) adding a support interface, or **c** changing the geometry
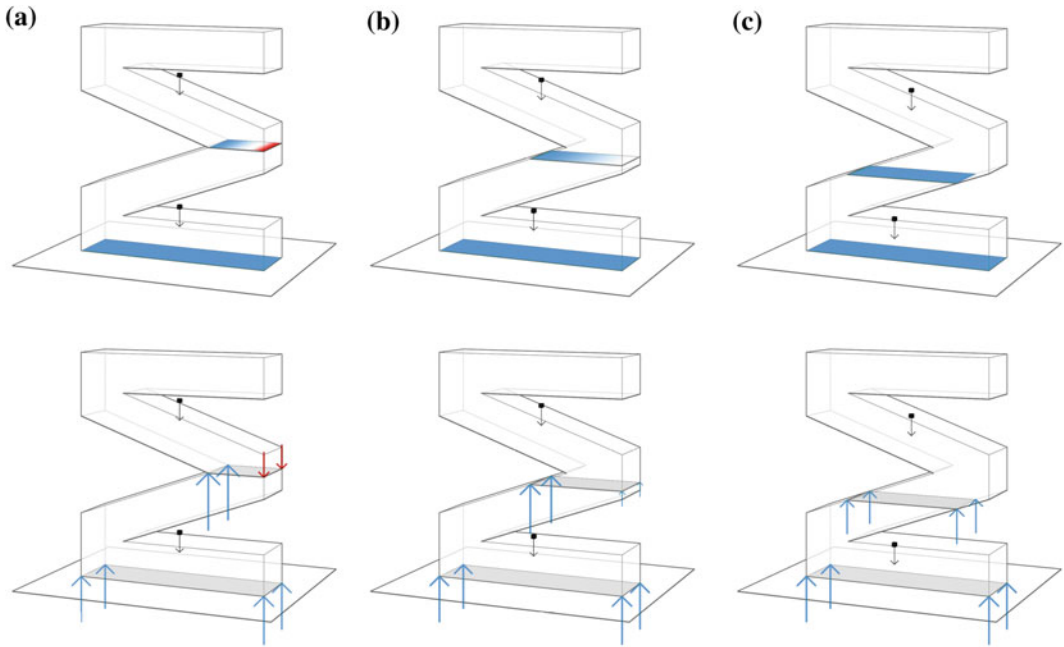
Fig. 4 Tension forces at the internal interfaces (**a**) can be removed by changing the location of the interface (**b**). More robust solutions are recognized by more uniform colouring of the interfaces (**c**)
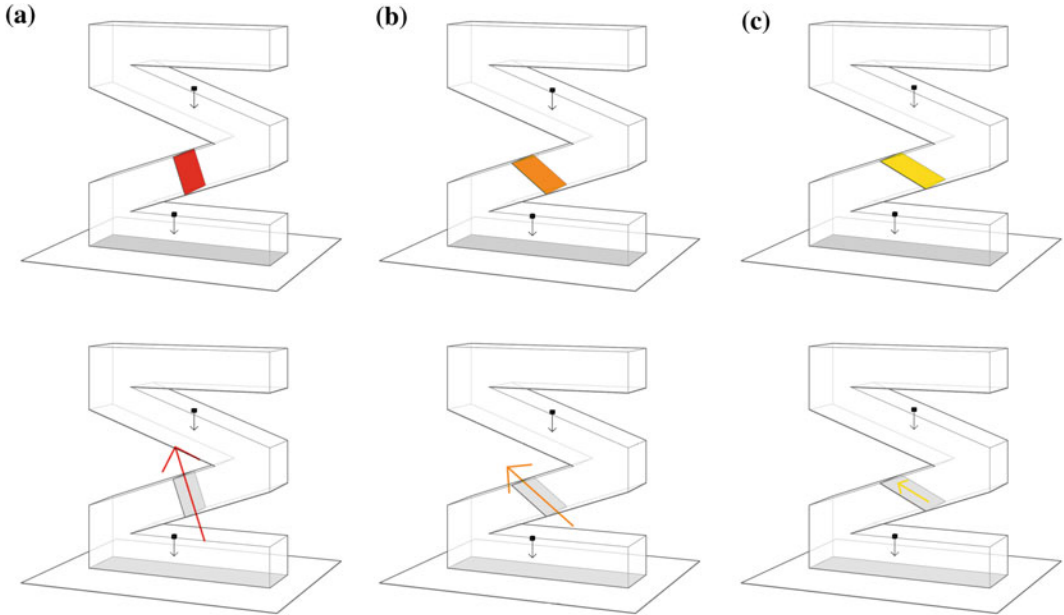
Fig. 5 Violation of friction limitations at an internal interface (**a**) can be resolved by, for example, rotation of that interface (**b**). The amount of friction is indicated by a colour ranging from *yellow* to *red*. *Red* indicates that maximum friction is exceeded (**a**). *Yellow* indicates that friction is below a user-defined threshold (**c**)

zb61 clear binder and impregnated with Z-Bond 101. The density of the composite material has been approximated with 0.60 g/cm^3, and the frictional angle of 40° (Van Mele et al. 2012). All interfaces have been modeled flat and planar in the computational and physical models, to not change the frictional behaviour between them. This means no male-female interlocking mechanisms have been used, for example to assist during the assembly process.

Case Study One

Figure 6 shows two different decompositions of the DMSC acronym of the symposium. In both cases, we started from one solid geometry, separated the letters where possible, and then further discretized the letters into smaller pieces. All cuts were positioned and adjusted manually, based on the visual feedback of the equilibrium calculations. Figure 6b, c depict the tension-compression and frictional contact forces at all interfaces. Both assemblies require compressive and frictional forces for equilibrium. Friction does not occur at the support interfaces.

A physical test with a 3D-printed model demonstrates the designed assembly is indeed stable by itself without any mechanical connections or glue (Fig. 1).

Note that the process of assembling the model was difficult, because interim stability during assembly was not considered in the design of the decomposition. In fact, equilibrium could not be achieved for the combination of "D" and "M" alone, without the additional weight of the letters "S" and "C".

Case Study Two

This case study demonstrates the potential of the proposed interactive procedure to explore a variety of equilibrium solutions for the same given initial shape (Fig. 7). As can be seen in Fig. 7a, the initial shape for this case study is a threedimensional, kinked loop positioned on a horizontal plane. The initial geometry is in equilibrium, with evenly distributed compression forces at the support.

In Fig. 7b, the object has been partitioned into two L-shaped and two cuboid geometries by four horizontal cuts. The corresponding interface-force diagrams illustrate that the thereby generated assembly is stable. All interface forces are compressive and vertical. No friction is required to establish equilibrium.

Even after further decomposition with vertical cuts through the L-shaped elements, the assembly remains self-supporting (Fig. 7c). All interface forces are still compressive and vertical. Therefore, as before, no friction is required. Furthermore, there is no force interaction on the two vertical interfaces. The assembly could thus be separated into two independent parts and remain stable.

A completely different decomposition is achieved with inclined cuts, as seen in Fig. 7d. In terms of force transfer, this configuration is more interesting. It requires both compressive and friction forces to be in equilibrium, because arch action is activated by the orientation of the cuts.

The physical models in Fig. 8 demonstrate that the designed assemblies of this case study are indeed stable by themselves.

Case Study Three

Figure 9 shows the outcome of a completely different decomposition strategy. Starting with a simple box with an open bottom, a decomposition pattern has been applied on the outer box surface. From that cutting pattern (Fig. 9a), interface geometries with the potential to self-interlock in an assembly have been generated. This has been achieved through extrusion of the cutting pattern to a single point. Therefore, the resulting interfaces are planar and conical directed to that point. The contact-force diagrams in Fig. 9a illustrate that the assembly is self-supporting. All contact forces are either compressive or frictional and the maximum friction is not exceeded.

Fig. 6 Two different decompositions of the DMSC acronym (*left*), with the corresponding interface-force diagrams in compression-tension mode (*middle*) and friction mode (*right*)
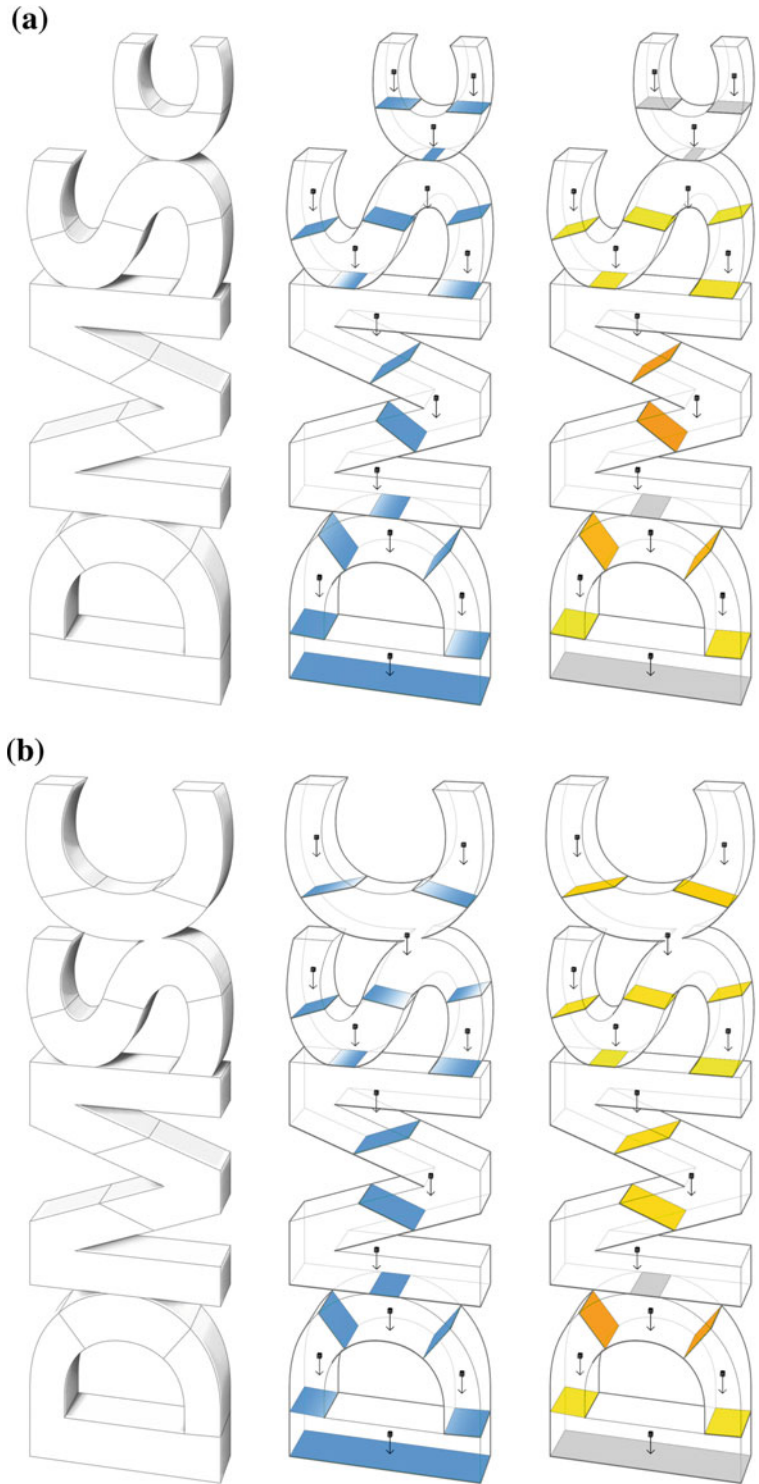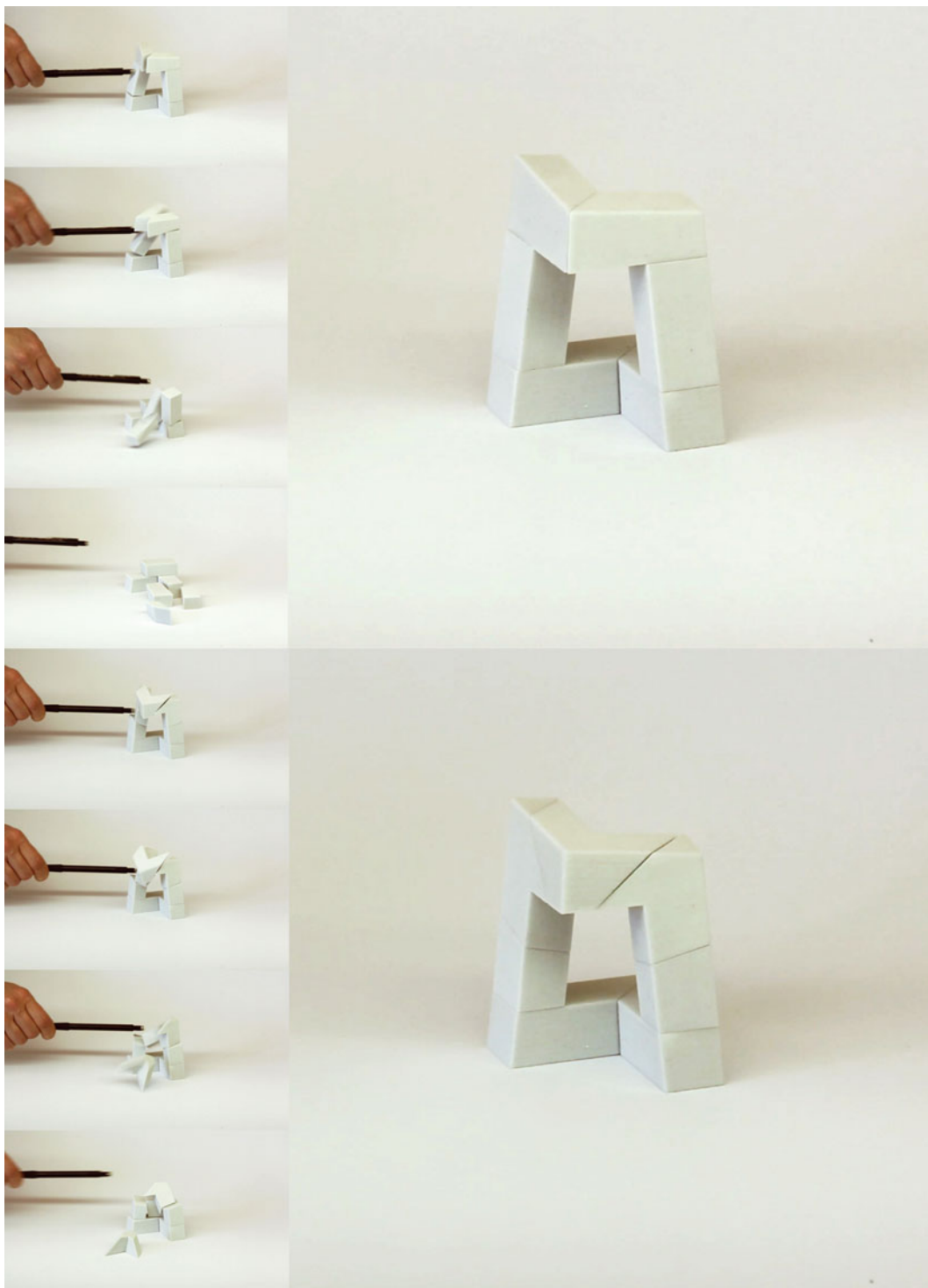
Fig. 7 Various equilibrium solutions for the same initial geometry (*left*), with the corresponding interface-force diagrams in compression-tension mode (*middle*) and friction mode (*right*)
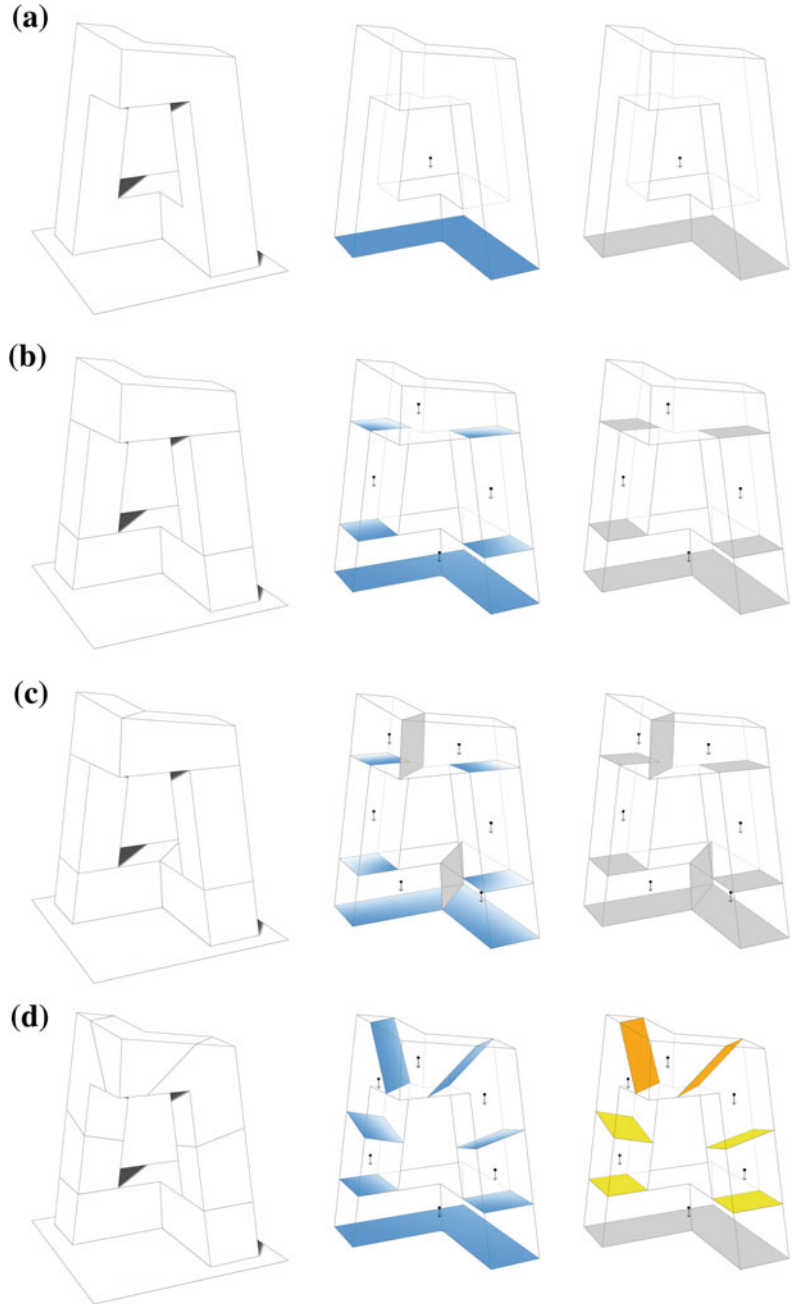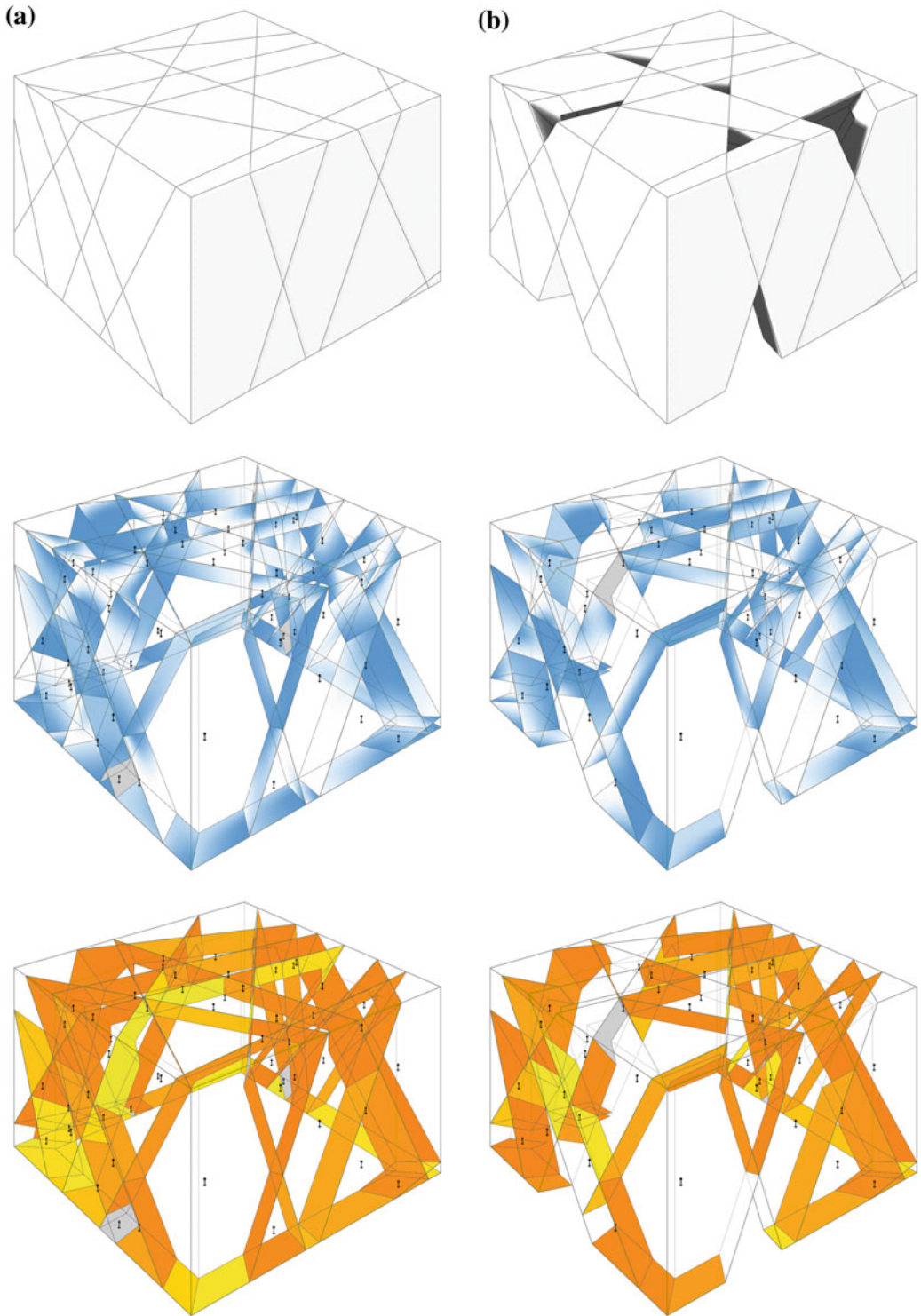
Furthermore, even after removing several parts of the assembly, as seen in Fig. 9b, the resulting configuration remains in self-supporting equilibrium. Again, the physical models in Fig. 10 demonstrate the self-supporting equilibrium of the designed decompositions.

Fig. 8 Photographs of two different decompositions from the same initial geometry

Fig. 9 Resulting decomposition of case study three before (*top* **a**) and after removing several parts of the assembly (*top* **b**), with the corresponding interface-force diagrams in compression-tension mode (*middle*) and friction mode (*bottom*)
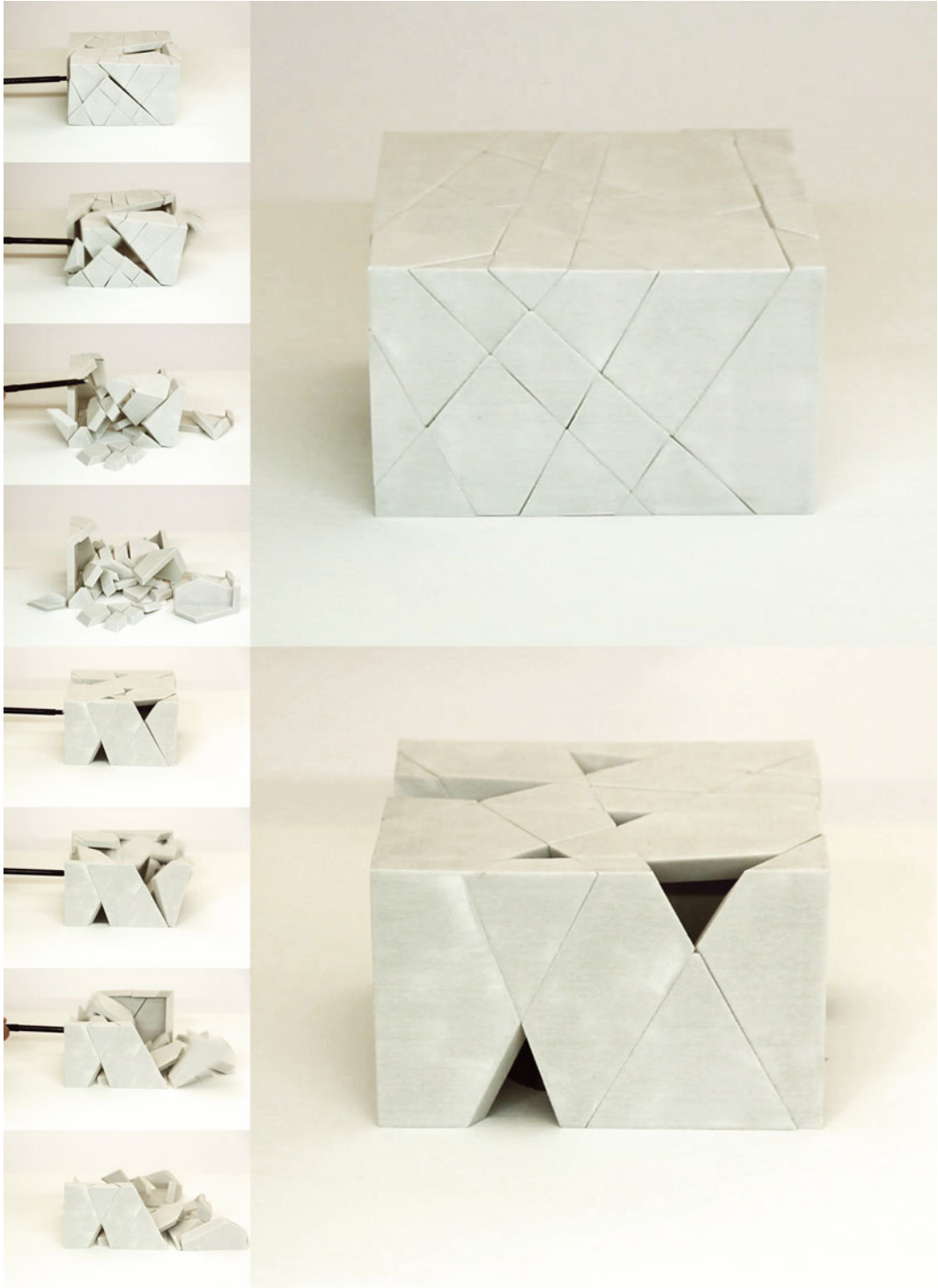
Fig. 10 Photographs of case study three before (*top*) and after removing parts from the assembly (*bottom*)

Conclusion

In practice, volumetric decomposition into self-supporting assemblies has applications in areas ranging from the construction of large-scale, cut-stone masonry structures (Howeler et al. 2014) and prefabricated building assemblies, to smaller-scale prototyping. When applied to the design and production of prefabricated elements in the building industry, optimization of joints can be achieved as a means of limiting joinery to predominantly no-tension force transfer.

The prototypical decomposition tool presented in this paper is based on realtime, clear, visual feedback. The advantage of such an interactive process has been demonstrated through the surprising results shown in "*Results*". As can be seen in those case studies, the step-by-step, interactive discretization process has successfully been used to explore the design space of discrete-element assemblies and experiment with previously unseen forms.

Despite the promising results shown in "*Results*", the interactive decomposition procedure can be time consuming and the handling of large models can be problematic. Further research will be necessary to develop general, (semi-)automated decomposition strategies. A digital self-supporting equilibrium solution does not automatically guarantee a physical self-supporting application. As explained in previous research (Whiting 2012), an alternative equilibrium state could exits where friction constraints are violated. Furthermore, the implemented algorithms do not consider imperfections of element's geometry or assembly.

This research is part of a larger research project, which aims to develop better understanding and novel techniques for the equilibrium design of masonry and other discrete-element assemblies. Near-future goals related to the research presented are the implementation of additional methods for the equilibrium design, such as manipulation of weight distribution within the volume (Bacher et al. 2014), and the development of general, automatic decomposition strategies. Furthermore, the research will focus on the structural integrity and robustness by considering possible material failure at unit scale and interim stability during assembly.

References

Bächer M, Whiting E, Bickel B, Sorkine-Hornung O (2014) Spin-it: optimizing moment of inertia for spinnable objects. ACM Trans Graph 33(4):96:1–96:10

Bullet-Physics-Libary (Copyright (c) 2012) Bullet collision detection and physics library. http://bulletphysics.org

Deuss M, Panozzo D, Whiting E, Liu Y, Block P, Hornung-Sorkine O, Pauly M (2014) Assembling self-supporting structures. ACM Trans Graph 33(6):214:1–214:10

Eigensatz M, Kilian M, Schiftner A, Mitra NJ, Pottmann H, Pauly M (2010) Paneling architectural freeform surfaces. ACM Trans Graph 29(4):45:1–45:10

Grasshopper (Copyright 2009) Grasshopper—algorithmic modeling for rhino version 27 August 2014. http://www.grasshopper3d.com

Höweler E, Yoon JM, Ochsendorf J, Block P, DeJong M (2014) Material computation—the collier memorial design using analog and digital tools. In: Gerber DJ, Ibaez M (eds) Paradigms in computing—making, machines and models for design agency in architecture, chapter 0. eVolo Press, Los Angeles

Hu R, Li H, Zhang H, Cohen-Or D (2014) Approximate pyramidal shape decomposition. ACM Trans Graph 33(6):213:1–213:12

Livesley RK (1978) Limit analysis of structures formed from rigid blocks. Int J Numer Meth Eng 12:1853–1871

Livesley RK (1992) A computational model for the limit analysis of threedimensional masonry structures. Meccanica, 27(3):161–172. Nvidia-PhysX (Copyright 2013)

Nvidia physx library (2013). http://www.nvidia.com/object/physx-9.12.0213-driver.html

Panozzo D, Block P, Sorkine-Hornung O (2013) Designing unreinforced masonry models. ACM Trans Graph 32(4):91:1–91:12

Pottmann H, Schiftner A, Bo P, Schmiedhofer H, Wang W, Baldassini N, Wallner J (2008) Freeform surfaces from single curved panels. ACM Trans Graph 27(3):76:1–76:10

Python (Copyright 2001–2015) Python programming language. https://www.python.org

Rhinoceros (Copyright 1993–2014) Rhinoceros modeling tools for designers, version 5. https://www.rhino3d.com

Rippmann M, Curry J, Escobedo D, Block P (2013) Optimising stonecutting strategies for freeform masonry vaults. In: Proceedings of the international association for shell and spatial structures (IASS) symposium 2013. Wroclaw, Poland

Van Mele T, McInerney J, DeJong M, Block P (2012) Physical and computational discrete modeling of masonry vault collapse. In: Proceedings of the 8th international conference on structural analysis of historical constructions. Wroclaw, Poland

Whiting E, Ochsendorf J, Durand F (2009) Procedural modeling of structurally-sound masonry buildings. ACM Trans Graph 28(5):112

Whiting E, Shin H, Wang R, Ochsendorf J, Durand F (2012) Structural optimization of 3d masonry buildings. ACM Trans Graph 31(6):159:1–159:11

Whiting EJW (2012) Design of structurally-sound masonry buildings using 3d static analysis. PhD thesis, Department of Architecture, Massachusetts Institute of Technology